Sharp Curve Lane Boundaries Projective Model and Detection

Yong Chen
School of Software and Microelectronics
Shaanxi Prov. Key Lab. of Inf. Acquisition & Processing
Northwestern Polytechnical University
Xi'an, Shaanxi, China

Mingyi He
Shaanxi Prov. Key Lab. of Inf. Acquisition & Processing
School of Electronics and Information
Northwestern Polytechnical University
Xi'an, Shaanxi, China

***Abstract*—An effective lane boundaries projective model (LBPM) and improved detection method in the images captured with a vehicle-mounted monocular camera in complex environments, especially for sharp circular curve lane, is proposed in this paper. Firstly, a lane boundaries projective model is deduced. This lane model can not only express straight-line lane boundaries, but also describe the actual sharp circular curve lane boundaries very well. Secondly, the lane posterior probability function is derived by employing the lane model, the gradient direction feature, the lane likelihood function, and the lane prior information. And then the lane maximum posteriori probability is found out by using the improved particle swarm optimization algorithm. Further the lane boundaries is positioned, and the lane geometric structure, such as the lane left and right boundaries curve radiuses, can be calculated accurately through the lane model. The experimental results show that the proposed lane boundaries projective model and the improved detection method are more effective and accurate for sharp curve lane detection.**

Keywords-lane detection; lane model; lane likelihood function; lane posterior probability

I. INTRODUCTION

Structural lane detection in road images is a primary, essential, and important component of many intelligent vehicle applications, such as intelligent vehicle control, intelligent cruise, lane departure warning, autonomous driving, *etc* [1]. In order to warn driver about the dangerous situations of lane departure, or make decisions and take control of the vehicle to avoid danger without delay, the lane boundaries must be detected accurately and effectively for a variety of lane alignments and complex road environments. The research is active and extensive in intelligent transportation during the past decade. But there are many problems need to be solved in lane detection. One of them is sharp curve lane detection.

The sharp curve lane model in images is primary for sharp curve lane detection. Many lane models have been proposed based on different hypotheses of lane alignments in the last few years. The lane is modeled as straight line in [2] and [3], which cannot be used in curve lane detection. Many lane models utilized in [4-9] are modeled with spline curve, or a series of circular arcs, complex clothoid, parabolic curve, *etc*. These lane models can be used to fit curve lane boundaries in some extent, but they cannot give out the geometric parameters about the curve lane. The parametric model of the lane projection on the image plane is employed in [1] and [10-12], but it does not meet sharp curve lane completely, there is large error between it and the actual sharp curve lane boundary.

An accurate and effective lane boundaries projective model (LBPM) and detection method is proposed to tackle the above problem in this paper. The LBPM is more precise for sharp curve lane. With the aim of describing the straight line and circular curve lane shape in detail, we go through the lane boundaries model on the image plane. And then the lane likelihood function is gotten by using the gradient direction feature. Subsequently the prior knowledge of lane width and the constraints of the LBPM parameters are converted to the lane priori probability, and the lane posterior probability function is held based on Bayesian formula. Capitalizing on the function, we utilize the improved particle swarm optimization algorithm to get the lane maximum posterior probability. Thereby the lane left and right boundaries are located.

The LBPM and the lane posterior probability function proposed in this paper are different and distinguished from ones in the previous literatures [1] [10-12]. The circular lane left and right boundaries curve radiuses are normally assumed to be the same as each other in those literatures. The assuming is not in conformity with the actual circular curve lane. But our LBPM can accurately describe the actual straight lane and circular curve lane. And the lane posteriori probability function based on the LBPM is more reasonable.

II. PROJECTION MODEL OF CURVE LANE

Highway alignment on plan is composed of three kinds of alignment elements, straight line, circular curve, and clothoid pursuant to the technical standard of highway engineering [13]. Let C_0 denotes the lane curvature at the starting point, C_1 denotes the curvature change rate of lane curve, and assume the road surface is planar. Then the lane curvature C varies with the lane length l as $C(l) = C_0 + C_1 l$ [14]. As $C_1 \ll C_0$ [13] for the highway, lane curve can approximately be regarded as circular arc in the visual distance for stopping vehicle.

A. Lane Left Boundary Parametric Eq. in WCS

We build up the world coordinate system (WCS)

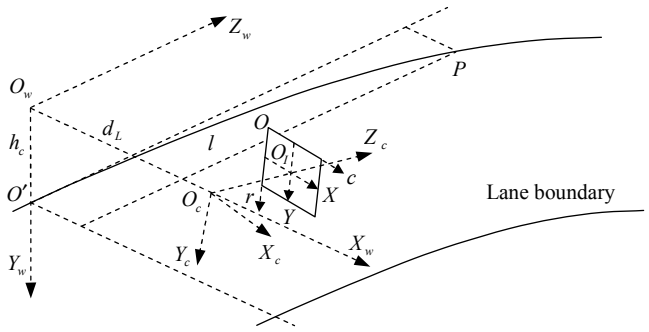

Figure 1. The coordinate systems for the lane boundary.

$O_wX_wY_wZ_w$ for circular curve lane as shown in Fig. 1, where the plane $O_wX_wZ_w$ is parallel to the road plane and its height above the road plane is the same as the height of the on-vehicle camera above the road plane, the axis O_wX_w passes through the camera centre, the axis O_wY_w intersects the lane left boundary at the point O', the axis O_wZ_w is parallel with the lane left boundary tangent line at the point O' [11].

Let P denotes a point on the lane left boundary, θ denotes the included angle between the plane $O_wY_wZ_w$ and the lane left boundary at the point P, l denotes the curve length from the point O' to the point P, $R_{lane,L}$ denotes the circular lane left boundary curve radius. Then $\theta = l/R_{lane,L}$, and when the lane is straight, $R_{lane,L} = \infty$ and $\theta = 0$. Let h_c denotes the distance from the point O' to the point O_w, which is the camera height above the road plane. Considering the minimum radius of lane circular curve is much larger than l in the visual distance [13], $\sin\theta \approx \theta$ and $\cos\theta \approx 1$, we derive the lane left boundary parametric equation in the WCS as follows

$$\begin{cases} x_w \approx l^2/\left(2R_{lane,L}\right) \\ y_w = h_c \\ z_w \approx l \end{cases} \tag{1}$$

B. Lane Left Boundary Parametric Eq. in CCS

Assuming the on-vehicle camera points to the right ahead of the vehicle and the camera roll angle $\gamma = 0$, we establish the camera coordinate system (CCS) $O_cX_cY_cZ_c$ as shown in Fig. 1. Let d_L denotes the horizontal distance from the camera to the lane left boundary, α denotes the camera inclination angle, which is the included angle between the plane $O_wZ_wX_w$ and the camera optical axis O_cZ_c, β denotes the included angle between the lane direction and the vehicle direction, which is the included angle between the axis O_cZ_c and the plane $O_wY_wZ_w$ [11]. Considering the vehicle is driven along the lane, β is very small, $\cos\beta \approx 1$ and $\sin\beta \approx \beta$ [1], we derive the lane left boundary parameter equation in the CCS from (1) as follows

$$\begin{cases} x_c \approx l^2/\left(2R_{lane,L}\right) + d_L - \beta l \\ y_c \approx -d_L\beta\sin\alpha + h_c\cos\alpha - l\sin\alpha \\ z_c \approx d_L\beta\cos\alpha + h_c\sin\alpha + l\cos\alpha \end{cases} \tag{2}$$

C. Lane Left Boundary Equations in ICS & PCS

We establish the image coordinate system (ICS) O_Ixy and the pixel coordinate system (PCS) Ocr in the imaging plane as shown in Fig. 1, where the axis O_cZ_c intersects perpendicularly the plane O_Ixy at the point O_I [11]. Let (x, y) denotes the point coordinate in the ICS, (c, r) denotes the pixel coordinate in the PCS, d_x, d_y denote respectively the pixel physical sizes on the x and y axis directions, (c_O, r_O) represents the pixel coordinate of the point O_I, and f denotes the camera focal length. We derive the lane left boundary equation in the ICS as follows

$$\begin{aligned} x = {} & \frac{d_L\cos\alpha}{h_c}\left(y + f\tan\alpha\right) - \frac{f\beta}{\cos\alpha} \\ & + \frac{f^2 h_c}{2R_{lane,L}\cos^3\alpha}\left(y + f\tan\alpha\right)^{-1} \end{aligned} \tag{3}$$

And then we derive the lane left boundary equation in the PCS as follows

$$c = b_{1L}\left(r - r_C\right) + b_0 + b_{-1L}\left(r - r_C\right)^{-1} \tag{4}$$

where $r_C = r_O - \frac{f\tan\alpha}{d_y}$, $b_{1L} = \frac{d_y d_L\cos\alpha}{d_x h_c}$, $b_0 = c_O - \frac{f\beta}{d_x\cos\alpha}$, $b_{-1L} = \frac{f^2 h_c}{2d_x d_y R_{lane.L}\cos^3\alpha}$.

D. Unified Form of Lane Boundary Eq. & Constraint

Paying attention to $R_{lane,L}$ in the above equations, we can see that $R_{lane,L}$ is the left boundary curve radius of right curved lane and $R_{lane,L} \geq 0$. When we derive the left boundary equation of left curved lane, $b_{-1L} = -\frac{f^2 h_c}{2d_x d_y R_{lane.L}\cos^3\alpha}$. In order to unify the equations form of the lane model, we define $R_{lane,L} > 0$ when lane curves to the right and $R_{lane,L} < 0$ when lane curves to the left. The minus of $R_{lane,L}$ does not mean that the lane curve radius is negative except represents the left curving direction.

Similarly, we can derive the lane right boundary equation as the same form of the left one except that the parameters corresponding to b_{1L} and b_{-1L} are different from the ones of the lane left boundary equation. Let b_{1R} and b_{-1R} denote respectively the corresponding parameters of the lane right boundary

equation. Then $b_{1R} = \dfrac{d_y d_R \cos\alpha}{d_x h_c}$ and $b_{-1R} = \dfrac{f^2 h_c}{2 d_x d_y R_{lane.R} \cos^3\alpha}$, where d_R denotes the horizontal distance from the camera to the lane right boundary, $R_{lane,R}$ denotes the curve radius of the lane right boundary. When the lane is straight, $R_{lane,L} = R_{lane,R} = \infty$; when the lane is right curved, $R_{lane,L} > R_{lane,R} > 0$; when the lane is left curved, $0 > R_{lane,L} > R_{lane,R}$. And $R_{lane,L} - R_{lane,R} = W_{lane}$, where W_{lane} denotes the lane width. Thus we get the equation through b_{-1L} and b_{-1R} as follows

$$b_{-1R} - b_{-1L} = \frac{f_c^2 h_c W_{lane}}{2 d_x d_y R_{lane,L} R_{lane,R} \cos^3\alpha} \tag{5}$$

From the above equation, it can be seen that the smaller the lane curve radius and the sharper the lane is curved, the greater $(b_{-1R} - b_{-1L})$. As lane curve radius is greater than a specific value according to the highway design standard [13], let $R_{lane,\min}$ denotes the minimum, we have the constraint as follows

$$b_{-1R} - b_{-1L} \le \frac{f_c^2 h_c W_{lane}}{2 d_x d_y \left(R_{lane,\min} + W_{lane}\right) R_{lane,\min} \cos^3\alpha} \tag{6}$$

E. Lane Boundaries Projection Model

Summarizing the above discussion, we can get the lane boundary projection model as follows

$$\begin{cases} c_L = b_{1L}\left(r_L - r_C\right) + b_0 + b_{-1L}\left(r_L - r_C\right)^{-1} \\ c_R = b_{1R}\left(r_R - r_C\right) + b_0 + b_{-1R}\left(r_R - r_C\right)^{-1} \end{cases} \tag{7}$$

where (c_L, r_L) denotes the pixel coordinate of the point on the lane left boundary, (c_R, r_R) denotes the pixel coordinate of the point on the lane right boundary, the expressions of b_{1L}, b_{1R}, b_0, b_{-1L}, b_{-1R}, and r_C are respectively as follows

$$\begin{cases} b_{1L} = \left(d_y d_L \cos\alpha\right) / \left(d_x h_c\right) \\ b_{1R} = \left(d_y d_R \cos\alpha\right) / \left(d_x h_c\right) \\ b_0 = c_O - f\beta / \left(d_x \cos\alpha\right) \\ b_{-1L} = f^2 h_c / \left(2 d_x d_y R_{lane.L} \cos^3\alpha\right) \\ b_{-1R} = f^2 h_c / \left(2 d_x d_y R_{lane.R} \cos^3\alpha\right) \\ r_C = r_O - \left(f \tan\alpha\right) / d_y \end{cases} \tag{8}$$

The proposed LBPM is different from the previous ones [1] [10-12]. It is more close to the sharp curve lane than before. Fig. 2 shows the circular lane shapes respectively expressed by the LBPMs in the previous literatures and this paper, from which it can be seen that there is the great error between the previous LBPM and the actual circular lane, the smaller the lane curve radius and the farther the lane is from the camera, the greater the error. But there is not error in the proposed LBPM. It describes adequately the actual circular curve lane boundaries very well.

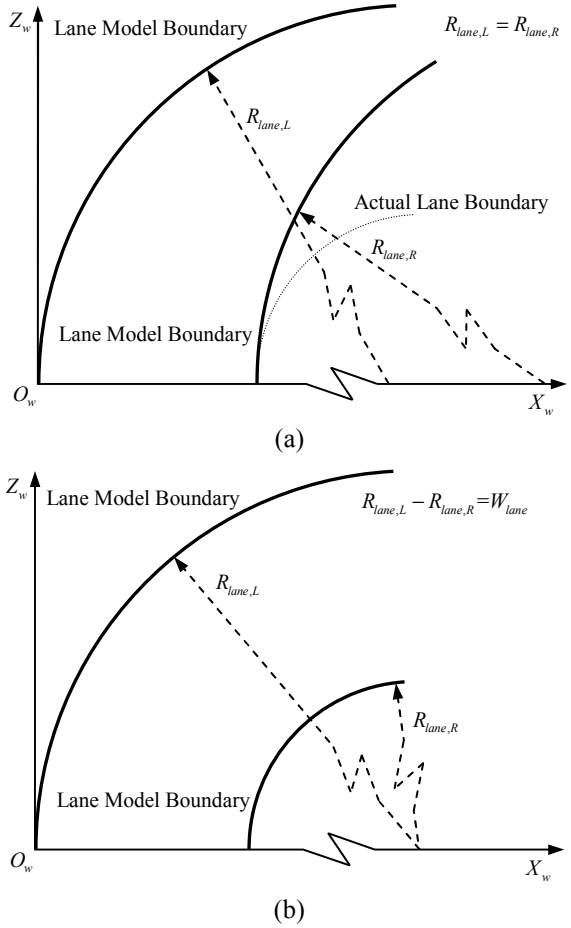

Figure 2. The lane shapes expressed by the previous and proposed LBPMs. (a) The lane shape plan by the previous LBPM. (b) The lane shape plan by the LBPM in this paper.

III. LANE FEATURES AND POSTERIORI PROBABILITY

Holding the LBPM is followed by extracting lane features from road image and estimating the lane boundary in road image. Naturally, before the estimating, we must derive the lane probability density function.

A. Lane Feature & Lane Likelihood Function

There are a variety of lane features can be used for lane detection, such as lane marking edge, edge gradient intensity, gradient direction, color, texture, frequency, *etc* [1-12], where the edge gradient direction feature [11] is good in anti-interference performance, algorithm cost, and computational complexity. It can suppress many kinds of interferences, such as shadows, sun glare, marking fading, *etc*, and enhance the robustness, accuracy, and efficiency of lane detection. Thus we use gradient direction feature to detect lane boundaries.

Let $\Theta(c,r)$ denotes the gradient direction of pixel point (c,r), $\mathbf{B} = \left(b_{1L}, b_{1R}, b_0, b_{-1L}, b_{-1R}\right)^T$ denotes the parameter vector

of the LBPM, $\phi(c,r)$ denotes the normal line direction of the LBPM at pixel point (c,r), which is a function of $\mathbf{B}$. Assuming the gradient direction observations of lane marking edge pixel point follow normal distribution with the variance σ_Θ^2 in the lane boundary neighborhood, we can derive the likelihood function of pixel point (c,r) as follows

$$p\left[(c,r)\,|\,\mathbf{B}\right] \propto \exp\left\{-\frac{\left[\Theta(c,r)-\phi(c,r)\right]^2}{2\sigma_\Theta^2}\right\} \tag{9}$$

Let $\boldsymbol{U}$ denotes the neighborhood of the LBPM curve, $\mathbf{I}_{GD}$ denotes the gradient direction image of the road image, and N_E denotes the image size. We derive the lane likelihood function as follows

$$p(\mathbf{I}_{GD}\,|\,\mathbf{B}) \propto \frac{1}{N_E}\sum_{(c,r)\in U}\exp\left\{-\frac{\left[\Theta(c,r)-\phi(c,r)\right]^2}{2\sigma_\Theta^2}\right\} \tag{10}$$

B. Lane Prior Information & Posterior Probability

For improving the accuracy of lane detection effectively, some lane prior information can be employed, such as lane width. As the lane width W_{lane} is constant for a specific lane according to the highway design standard [13], we can derive the equations through (8) as follows

$$b_{1R}-b_{1L}=\frac{d_y W_{lane}\cos\alpha}{d_x h_c} \tag{11}$$

$$\frac{1}{b_{-1L}}-\frac{1}{b_{-1R}}=\frac{2d_x d_y W_{lane}\cos^3\alpha}{f_c^2 h_c} \tag{12}$$

Supposing the observation of lane width W_{lane} is normally distributed, $(b_{1R}-b_{1L})$ and $\left(\frac{1}{b_{-1L}}-\frac{1}{b_{-1R}}\right)$ also follow normal distribution. Let μ_1, σ_1^2 and μ_{-1}, σ_{-1}^2 denote the means and variances of the distributions respectively, we can express the lane priori probability density function as follows

$$\begin{aligned} p(\mathbf{B}) \propto & \exp\left[-\left(b_{1R}-b_{1L}-\mu_1\right)^2\Big/\left(2\sigma_1^2\right)\right] \\ & \cdot\exp\left[-\left(\frac{1}{b_{-1L}}-\frac{1}{b_{-1R}}-\mu_{-1}\right)^2\Big/\left(2\sigma_{-1}^2\right)\right] \end{aligned} \tag{13}$$

Further we derive the lane posterior probability density function from (10) and (13) as follows

$$\begin{aligned} p(\mathbf{B}|\mathbf{I}_{GD}) \propto & \sum_{(c,r)\in U}\exp\left\{-\frac{\left[\Theta(c,r)-\phi(c,r)\right]^2}{2\sigma_\Theta^2}\right\} \\ & \cdot\exp\left\{-\frac{\left(b_{1R}-b_{1L}-\mu_1\right)^2}{2\sigma_1^2}-\left(\frac{1}{b_{-1L}}-\frac{1}{b_{-1R}}-\mu_{-1}\right)^2\Big/\left(2\sigma_{-1}^2\right)\right\} \end{aligned} \tag{14}$$

IV. LANE PARAMETERS OPTIMIZATION

With the above lane feature and the lane posterior probability density function, detecting lane in an image can be converted to estimating the LBPM parameters. Let $\hat{\mathbf{B}}$ denotes the maximum a posteriori estimation of $\mathbf{B}$, we express the process as follows

$$\begin{aligned} \hat{\mathbf{B}} = \arg\max_{\mathbf{B}} & \left\{\sum_{(c,r)\in U}\exp\left\{-\frac{\left[\Theta(c,r)-\phi(c,r)\right]^2}{2\sigma_\Theta^2}\right\}\right. \\ & \left.\cdot\exp\left\{-\frac{\left(b_{1R}-b_{1L}-\mu_1\right)^2}{2\sigma_1^2}-\left(\frac{1}{b_{-1L}}-\frac{1}{b_{-1R}}-\mu_{-1}\right)^2\Big/\left(2\sigma_{-1}^2\right)\right\}\right\} \end{aligned} \tag{15}$$

As there are several lanes and other interference in a road image, there are multiple extreme values in the posterior probability density function [4] [10] [11]. The traditional optimization methods cannot be used to evaluate the function maximum. Thus we utilize an improved particle swarm optimization algorithm to solve the problem.

Let m denotes the swarm size, define the particle search space as $\mathbf{S}=\left\{\mathbf{B}\,|\,\mathbf{B}_{\min}<\mathbf{B}<\mathbf{B}_{\max},\ \mathbf{B}_{\min},\mathbf{B}_{\max}\in R^5\right\}$, the fitness function $f(\mathbf{B})=p(\mathbf{B}|\mathbf{I}_{GD})$, $\mathbf{B}_i,\mathbf{V}_i,\mathbf{P}_i$, and $\mathbf{G}$ denote the i th particle position, velocity, best position, and the global best position respectively, where $i=1,2,\cdots,m$. And provide $\mathbf{V}_i$, $\mathbf{B}_i$, $\mathbf{P}_i$, and $\mathbf{G}$ are respectively updated in the $(k+1)$ th iteration as follows

$$\begin{aligned} \mathbf{V}_i(k+1) = & w(k)\mathbf{V}_i(k)+c_1 r_1\left[\mathbf{P}_i(k)-\mathbf{B}_i(k)\right] \\ & +c_2 r_2\left[\mathbf{G}(k)-\mathbf{B}_i(k)\right] \end{aligned} \tag{16}$$

$$\mathbf{B}_i(k+1)=\mathbf{B}_i(k)+\mathbf{V}_i(k+1) \tag{17}$$

$$\mathbf{P}_i(k+1)=\begin{cases}\mathbf{B}_i(k+1), & f\left[\mathbf{B}_i(k+1)\right]>f\left[\mathbf{P}_i(k)\right]\\ \mathbf{P}_i(k), & f\left[\mathbf{B}_i(k+1)\right]\le f\left[\mathbf{P}_i(k)\right]\end{cases} \tag{18}$$

$$\mathbf{G}(k+1)=\begin{cases}\mathbf{P}_{\max}(k+1), & f\left[\mathbf{P}_{\max}(k+1)\right]>f\left[\mathbf{G}(k)\right]\\ \mathbf{G}(k), & f\left[\mathbf{P}_{\max}(k+1)\right]\le f\left[\mathbf{G}(k)\right]\end{cases} \tag{19}$$

where $\mathbf{P}_{\max}(k+1)=\arg\max_{\mathbf{P}_i(k+1)} f\left[\mathbf{P}_i(k+1)\right]$, $w(k)$ is the inertia weight varying with the iterative times k, c_1 and c_2 are the learning factor, the values of which are taken as 2 in this work, r_1 and r_2 are the random numbers following the uniform distribution $U(0,1)$ [11] [15] [16].

The particles may fly out of the search space $\mathbf{S}$ during the optimization process. It causes the decline in the number of the particles valid searches and the degradation of the optimization algorithm performance. Although increasing the number of the particles search iterations could be used to solve the problem, it also increases greatly the computational cost. Thus we introduce a method to improve the number of the

Figure 3. The comparisons between experimental results with the proposed LBPM and the previous one. (a)-(c), (g)-(i), and (m)-(o) are the experimental results with the previous LBPM. (d)-(f), (j)-(l), and (p)-(r) are the experimental results with the proposed LBPM.

particles valid searches. When a particle flies out of the search space $\mathbf{S}$, it produces an offspring which is randomly put in the solution space, and then the particle dies out. In this way, not only the infeasible solution can be rejected, but also the particle search capability in feasible solution space can be enhanced without increasing the number of the particle search iterations.

V. Experimental Results

The lane detection method using the proposed LBPM is implemented with C++ program language. It costs about 300 milliseconds for processing one real road scene video image of size 512×288 pixels captured from the mounted camera by a PC with Pentium 4 CPU. To verify the effectiveness of our proposed LBPM and method, we test it with the sharp curve lane images in various complex road environments where some lane markings are partly blocked by other vehicles, or annoyed by the shadows and other markings. The experimental results and comparisons are given in Fig. 3. In these images, the sharp curve lane boundaries detected are signed by the red line. Fig. 3 (a)-(c), (g)-(i), and (m)-(o) are the experimental results of the sharp curve lane detection using the previous LBPM, where the large errors are marked by green ellipse line. Fig. 3 (d)-(f), (j)-(l), and (p)-(r) are the experimental results with the LBPM and detection method in this paper.

From the parts marked by green ellipse line, it can be seen that the previous LBPM leads to the large errors between the lane boundaries detected and the actual lane boundaries in the distant parts of the sharp curve lanes. However, compared with them, the lane boundaries detected with the method in this paper fit the actual lane boundaries very well. The experimental results demonstrate that the sharp curve lane detection with the proposed LBPM and method is more accurate and effective than the previous ones.

On the other hand, there are some limitations in the LBPM and improved detection method. It does not work well for the lane with great curvature change, and cannot detect any other lanes except the host lane.

VI. Conclusions

An effective LBPM and improved lane detection method in the images captured with a vehicle-mounted monocular camera in complex environments, especially for sharp circular curve lane, is proposed in this paper. Based on the LBPM, we introduce the lane posterior probability function employing the gradient direction feature, the lane likelihood function, and the lane prior information. After that, the maximum of the function is found out by using the improved particle swarm optimization. Further the lane boundaries are precisely positioned, and the lane geometric structure, such as the lane left and right boundaries curve radiuses, can be calculated accurately. The experimental results show that the proposed LBPM and the improved detection method are more effective and accurate for the sharp curve lanes. In the future, our study will focus on multi-lane detection.

Acknowledgment

This work is partially supported by the natural science foundation of China and the natural science foundation of Shaanxi Province.

References

[1] A. Guiducci, "Parametric model of the perspective projection of a road with applications to lane keeping and 3D road reconstruction," Computer Vision and Image Understanding, vol. 73, pp. 414-427, Mar. 1999.

[2] J. G. Wang, C. J. Lin and S. M. Chen, "Applying fuzzy method to vision-based lane detection and departure warning system," Expert Systems with Applications, vol. 37, pp. 113-126, 2010.

[3] A. Borkar, M. Hayes and M. T. Smith, "A novel lane detection system with efficient ground truth generation," IEEE Transactions on Intelligent Transportation Systems, vol. 13, pp. 365-374, 2012.

[4] K. Kluge, and S. Lakshmanan, "Deformable-template approach to lane detection," in Proceedings of the 1995 Intelligent Vehicles Symposium, pp. 54-59, 1995.

[5] J. W. Park, J. W. Lee and K. Y. Jhang, "A lane-curve detection based on an LCF," Pattern Recognition Letters, vol. 24, pp. 2301-2313, 2003.

[6] Y. Wang, E. K. Teoh and D. G. Shen, "Lane detection and tracking using B-Snake," Image and Vision Computing, vol. 22, pp. 269-280, 2004.

[7] K. Huh, J. Park, D. H. Hong, D. D. Cho, and J. H. Park, "Development of a vision-based lane detection system considering configuration aspects," Optics and Lasers in Engineering, vol. 43, pp. 1193-1213, 2005.

[8] Z. Kim, "Robust lane detection and tracking in challenging scenarios," IEEE Transactions on Intelligent Transportation Systems, vol. 9, pp. 16-26, Mar. 2008.

[9] J. Ruyi, K. Reinhard, V. Tobi, and W. Shigang, "Lane detection and tracking using a new lane model and distance transform," Machine Vision and Applications, vol. 22, pp. 721-737, 2011.

[10] Y. Zhou, R. Xu, X. F. Hu, and Q. T. Ye, "A robust lane detection and tracking method based on computer vision," Measurement Science and Technology, vol. 17, pp. 736-745, 2006.

[11] Y. Chen, M. Y. He and Y. F. Zhang, "Robust lane detection based on gradient direction," 6th IEEE Conference on Industrial Electronics and Applications (ICIEA), pp. 1547-1552, 2011.

[12] Y. F. Wang, N. Dahnoun and A. Achim, "A novel system for robust lane detection and tracking," Signal Processing, vol. 92, pp. 319-334, 2012.

[13] Ministry of Transport of the People's Republic of China, Technical Standard of Highway Engineering, JTG B01-2003. JAN. 29, 2004

[14] E. D. Dickmanns and B. D. Mysliwetz, "Recursive 3-D road and relative ego-state recognition," IEEE Transactions on Pattern Analysis and Machine Intelligence, vol. 14, pp. 199-213, 1992.

[15] Y. Shi and R. C. Eberhart, "Parameter selection in particle swarm optimization," Lecture Notes in Computer Science, vol. 1447, p. 591-591, 1998.

[16] P. K. Tripathi, S. Bandyopadhyay and S. K. Pal, "Multi-objective particle swarm optimization with time variant inertia and acceleration coefficients," Information Sciences, vol. 177, pp. 5033-5049, 2007.